

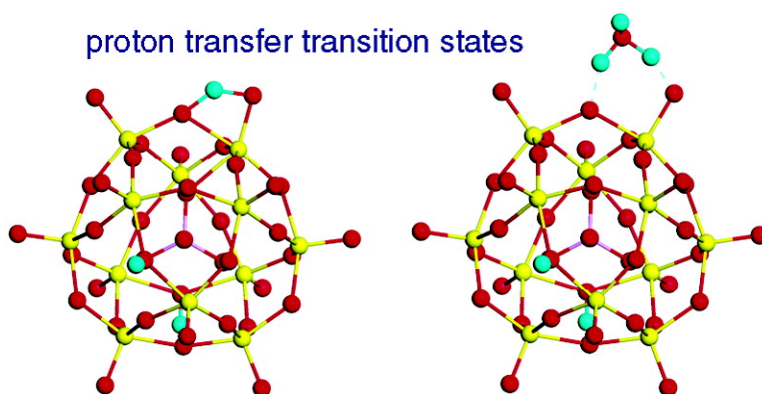
Article

Anhydrous and Water-Assisted Proton Mobility in Phosphotungstic Acid

Michael J. Janik, Robert J. Davis, and Matthew Neurock

J. Am. Chem. Soc., **2005**, 127 (14), 5238-5245 • DOI: 10.1021/ja042742o • Publication Date (Web): 16 March 2005

Downloaded from <http://pubs.acs.org> on March 25, 2009



More About This Article

Additional resources and features associated with this article are available within the HTML version:

- Supporting Information
- Links to the 3 articles that cite this article, as of the time of this article download
- Access to high resolution figures
- Links to articles and content related to this article
- Copyright permission to reproduce figures and/or text from this article

[View the Full Text HTML](#)

Anhydrous and Water-Assisted Proton Mobility in Phosphotungstic Acid

Michael J. Janik, Robert J. Davis, and Matthew Neurock*

Contribution from the Department of Chemical Engineering, University of Virginia, Charlottesville, Virginia 22904-4741

Received December 2, 2004; E-mail: mn4n@virginia.edu

Abstract: Nonlocal gradient-corrected density functional theoretical calculations were used to determine the energetics associated with proton migration in phosphotungstic acid. The activation energy for anhydrous proton hopping between two oxygen atoms on the exterior of the molecular Keggin unit was calculated to be 103.3 kJ mol⁻¹. The quantum-tunneling effect on the rate of proton movement was determined using semiclassical transition-state theory and was found to be a major contributor to the overall rate of proton movement at temperatures below approximately 350 K. The adsorption of water on an acidic proton decreases the activation barrier for hopping to 11.2 kJ mol⁻¹ by facilitating proton transfer along hydrogen bonds. The overall rate constant for proton hopping was determined as a function of temperature and water partial pressure. Small amounts of water greatly enhance the overall rate of proton movement.

Introduction

Heteropolyacids (HPAs) show promise as strong solid-acid catalysts and as proton-conducting materials for use in proton exchange membrane fuel cells. As strong solid acids, HPAs may provide an alternative to the toxic, corrosive liquid acids currently used for a reaction such as alkylation.^{1–4} The established technologies for refinery alkylation processes use large quantities of anhydrous hydrofluoric or sulfuric acid. Replacement of these liquid acids with a solid acid catalyst will alleviate environmental safety concerns associated with the homogeneous processes. As a proton-conducting material, HPAs exhibit high conductivity^{5,6} and can be incorporated in composite membranes for use in proton exchange membrane (PEM) fuel cells.^{7–10} Understanding the influence of water on the reactivity and proton conductivity of HPAs is essential to advance the use of HPAs as solid-acid catalysts and as additives in PEM fuel cells.

The basic unit of the heteropolyacid is the heteropolyanion. Keggin structures (XM₁₂O₄₀ⁿ⁻) are the most commonly studied heteropolyanions because of their greater acid strength, stability, and availability compared to those of other polyoxometalates. A Keggin unit is illustrated in Figure 1. The strongest acid among the common Keggin units is phosphotungstic acid^{11,12}

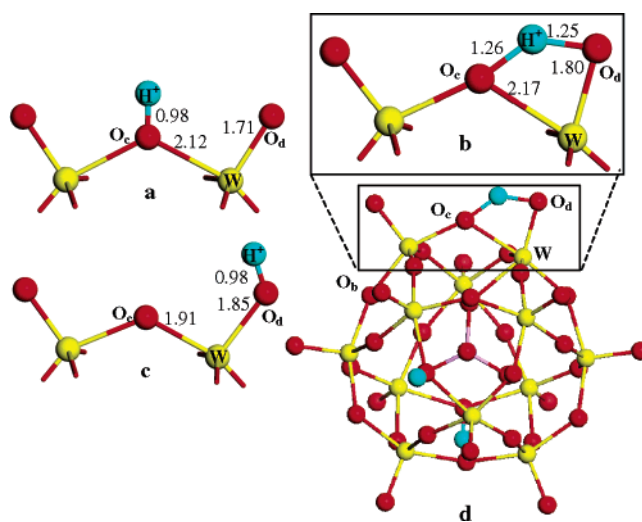


Figure 1. DFT calculated equilibrium states and transition state for the proton-hopping reaction between an O_c atom and an O_d atom of HPW. (a) Equilibrium structure with H⁺ bound to an O_c atom. (b) Transition state for the proton-hopping reaction between O_c and O_d atoms. (c) Equilibrium structure with H⁺ bound to an O_d atom. (d) Full Keggin unit view of the transition state. All calculations were performed on the full Keggin unit. The ZPVE corrected activation energy for movement starting on the O_c oxygen atom is 103.3 kJ mol⁻¹. The ZPVE corrected reaction energy for proton hopping from the O_c to O_d oxygen atom is 12.4 kJ mol⁻¹. Geometric parameters are given in Table 1. Distances are given in Å.

(HPW) in which the central (X) atom is phosphorus and the addenda (M) atoms are tungsten (i.e., PW₁₂O₄₀³⁻). Protons coordinate to oxygen atoms on the exterior of the Keggin unit (KU) to complete the primary structure of the heteropolyacid.

Adsorption of water molecules to the acidic protons of HPW is exothermic.¹² Adsorbed water molecules hydrogen bond with

- (1) Kozhevnikov, I. V. *Russ. Chem. Rev.* **1987**, *56*, 811–825.
- (2) Okuhara, T.; Mizuno, N.; Misono, M. *Adv. Catal.* **1996**, *41*, 113–252.
- (3) Misono, M. *C. R. Acad. Sci., Ser. II: Chim.* **2000**, *3*, 471–475.
- (4) Misono, M. *Chem. Commun.* **2001**, 1141–1152.
- (5) Nakamura, O.; Kodama, T.; Ogino, I.; Miyake, Y. *Chem. Lett.* **1979**, 17–18.
- (6) Slade, R. C. T.; Barker, J.; Pressman, H. A.; Strange, J. H. *Solid State Ionics* **1988**, *28–30*, 594–600.
- (7) Malhotra, S.; Datta, R. *J. Electrochem. Soc.* **1997**, *144*, L23–L26.
- (8) Kim, Y. S.; Wang, F.; Hickner, M.; Zawodzinski, T. A.; McGrath, J. E. *J. Membr. Sci.* **2003**, *212*, 263–282.
- (9) Tazi, B.; Savadogo, O. *Electrochim. Acta* **2000**, *45*, 4329–4339.
- (10) Ramani, V.; Kunz, H. R.; Fenton, J. M. *J. Membr. Sci.* **2004**, *232*, 31–44.
- (11) Bardin, B. B.; Bordawekar, S. V.; Neurock, M.; Davis, R. J. *J. Phys. Chem. B* **1998**, *102*, 10817–10825.

- (12) Janik, M. J.; Campbell, K. A.; Bardin, B. B.; Davis, R. J.; Neurock, M. *Appl. Catal. A* **2003**, *256*, 51–68.

oxygen atoms of nearby KUs, linking the units together to form a secondary structure. The hydration level of phosphotungstic acid is a function of temperature and relative humidity, with the hexahydrate ($\text{H}_3\text{PW}_{12}\text{O}_{40}\cdot 6\text{H}_2\text{O}$) being stable at room temperature and low relative humidity.^{13,14} Dehydration of the hexahydrate species begins just above room temperature and continues above 500 K.¹¹ The energy for water desorption and the effect of desorption on the bulk structure and proton position were previously studied using quantum-chemical methods.¹⁵

The adsorption of water molecules on acidic protons is generally considered to poison an acid catalyst by reducing the acid strength. However, upon increasing the hydration level of HPW, the activity for cyclopropane isomerization was shown to initially increase before significantly decreasing.¹⁶ This initial enhancement was speculated to be caused by increased proton mobility. The decrease in activity at higher hydration levels then results from a decrease in acid strength. In addition, the catalytic activity of HPW under dry conditions declined with time on stream for butene double bond isomerization and pentane skeletal isomerization, whereas treatment with water vapor substantially recovered the catalytic activity.¹⁷ An increase in proton mobility from small amounts of water may account for the enhancements in catalytic performance. Indeed, Baba and Ono suggested that the dynamic properties of protons may be vital to solid-acid catalysis.¹⁶

Proton-conductivity studies of HPW also recognize the importance of water in enhancing the proton mobility. The conductivity was found to decrease with decreasing hydration levels from 21 to 14 to 6 water molecules per KU.⁶ The effect of water on the proton conductivity of HPAs is pertinent to their use in the membranes of PEM fuel cells. High-temperature (>393 K) operation of PEM fuel cells is desired to improve the CO tolerance of the Pt electrode, increase the reaction rates, manage the water more efficiently, and simplify system integration.¹⁸ Heteropolyacids have been explored as additives to materials such as Nafion to increase their water retention at high temperatures and increase their proton density.^{7–10} Improved understanding of the mechanism of water-enhanced mobility and the factors that affect water desorption will help determine the optimal design and operation of fuel cells with HPA-containing proton-exchange membranes.

The elementary step for proton motion is the proton-transfer or proton-hopping reaction, in which a proton moves from one oxygen atom to another along the exterior surface of a single KU. In this study, density functional theory quantum-chemical methods are used to determine the energetics associated with elementary proton-hopping paths. The reaction and activation energies are determined for both the anhydrous and water-assisted proton-hopping processes. In the presence of low amounts of water, the mobility of hydrated protons is dominated by movement as H_3O^+ , which is termed the vehicle mechanism.¹⁹ Statistical mechanics and conventional transition-state theory are used, together with the theoretically calculated

energies, to determine the rate constants with and without water assisting the proton motion. The effect of quantum tunneling on the anhydrous rate constant is estimated using semiclassical transition-state theory as developed by Fermann and Auerbach.²⁰ The theoretical results are used to determine the water adsorption equilibrium constant which is used along with the individual rate constants to predict the overall rate constant for proton hopping as a function of temperature and the amount of water present.

Computational Methods

Quantum-chemical calculations were performed using gradient-corrected density functional theory as implemented in the Vienna ab initio Simulation Package (VASP) using plane-wave basis sets.^{21–23} Ultrasoft pseudopotentials were used to describe electron–ion interactions.²⁴ Exchange and correlation energies were calculated using the Perdew–Wang (PW91) form of the generalized gradient approximation.²⁵ A cutoff energy of 396.0 eV for the plane-wave basis set was used in all calculations. A $1 \times 1 \times 1$ Monkhorst–Pack mesh was used to sample the first Brillouin zone.²⁶ This method has previously been shown to determine an equilibrium Keggin structure in agreement with experiment.¹²

All calculations were performed on the complete phosphotungstic KU along with three protons. The molecular system was represented within the periodic code by using a $20 \times 20 \times 20 \text{ \AA}^3$ unit cell with 8 \AA of vacuum space between Keggin units in adjacent supercells. Optimized geometries were located using a quasi-Newton forces minimization algorithm.

The nudged elastic band transition-state search method was used within VASP to isolate transition states.²⁷ This method involves optimizing a chain of images that connect the reactant and product states to determine the minimum energy reaction path. The nuclear positions are optimized with the constraint of only moving perpendicular to the current hyper-tangent, defined as the normal vector between the two neighboring images. The transition state is then identified as the maximum energy image. For the proton-hopping reaction, four initial images were linearly interpolated between reactants and products. A transition state was identified as the image with a maximum in energy and a tangential force less than 0.08 eV \AA^{-1} . The forces on this image were then separately optimized to remove any artificial forces introduced by the constraints of the elastic band method.

The harmonic vibrational modes were determined for equilibrium and transition states. Positive and negative displacements of 0.01 \AA in each of the Cartesian coordinates were used to determine the Hessian matrix. The use of “constrained” vibrational calculations was explored, in which the Hessian matrix is determined only for those atoms involved in the proton-hopping reaction. Transition states were confirmed by the presence of a single imaginary frequency along the reaction coordinate mode. Vibrational frequencies were used to calculate zero-point vibrational energy (ZPVE) corrections.

Overall rates of the proton-hopping reaction were computed using transition-state theory and statistical mechanics, following the same approach as Ryder et al. for the study of the proton-hopping reaction in H-ZSM-5.²⁸ For the anhydrous proton-hopping reaction, the rate constant per proton is calculated as

$$k^{\text{TST}} = \left(\frac{k_{\text{B}}T}{h} \right) \frac{q_{\text{TS,vib}}}{q_{\text{H}^+ - \text{initial,vib}}} e^{-E_{\text{act}}/RT} \quad (1)$$

(13) Nakamura, O.; Ogino, I.; Kodama, T. *Mater. Res. Bull.* **1980**, *15*, 1049–1054.

(14) Nakamura, O.; Ogino, I.; Kodama, T. *Solid State Ionics* **1981**, *3–4*, 347–351.

(15) Janik, M. J.; Davis, R. J.; Neurock, M. *J. Phys. Chem. B* **2004**, *108*, 12292–12300.

(16) Baba, T.; Ono, Y. *Appl. Catal. A* **1999**, *181*, 227–238.

(17) Bardin, B. B.; Davis, R. J. *Appl. Catal. A* **2000**, *200*, 219–231.

(18) Yang, C.; Costamangna, P.; Srinivasan, S.; Benziger, J.; Bocarsly, A. B. *J. Power Sources* **2001**, *103*, 1–9.

(19) Kreuer, K. D. In *Proton Conductors: Solids, Membranes and Gels – Materials and Devices*; Colomban, P., Ed.; Chemistry of Solid State Materials, Vol. 2; Cambridge University Press: Cambridge, 1992; pp 474–486.

(20) Fermann, J. T.; Auerbach, S. A. *J. Chem. Phys.* **2000**, *112*, 6787–6794.

(21) Kresse, G.; Hafner, J. *Phys. Rev. B* **1993**, *47*, 558–561.

(22) Kresse, G.; Furthmüller, J. *Comput. Mater. Sci.* **1996**, *6*, 15–50.

where h is Planck's constant, k_B is Boltzmann's constant, E_{act} is the ZPVE corrected activation barrier, R is the universal gas constant, and T is the temperature. The ratio of the vibrational partition functions, q_{vib} , of the transition state and equilibrium initial state appears in the preexponential factor. Similarly, for the water-assisted proton-hopping reaction, the rate per H_3O^+ species is

$$k^{\text{TST}} = \left(\frac{k_B T}{h} \right) \frac{q_{\text{TS,vib}}}{q_{\text{H}_3\text{O}^+ - \text{initial,vib}}} e^{-E_{\text{act}}/RT} \quad (2)$$

Quantum-tunneling transitions may represent a substantial fraction of anhydrous proton-hopping reactions. The importance of quantum tunneling to the anhydrous proton-hopping rate was determined using the semiclassical transition-state theory (SC-TST) as developed by Fermann and Auerbach;²⁰

$$k^{\text{SC-TST}} = k^{\text{TST}} \left[\frac{e^{E_{\text{act}}/RT}}{1 + e^{2\pi E_{\text{act}}/\hbar|\omega|}} + \frac{1}{2} \int_{-\infty}^{\pi E_{\text{act}}/\hbar|\omega|} e^{\hbar|\omega|\theta/\pi k_B T} \text{sech}^2 \theta \, d\theta \right] = k^{\text{TST}} \Gamma(T) \quad (3)$$

where k^{TST} is defined in eq 1, N is Avogadro's number, θ is the barrier penetration integral for the reaction coordinate, and ω is the imaginary harmonic frequency associated with the curvature at the top of the barrier. The rate is defined as the classical transition-state theory rate constant, k^{TST} , multiplied by a tunneling correction factor, $\Gamma(T)$, which is shown in brackets in eq 3. A numerical scheme is used to evaluate the integral in eq 3. This expression was derived from harmonic semiclassical transition-state theory by reintroducing the ground state of reactants for the low-energy limit of the barrier penetration integral. This method was chosen because it requires calculation of the energy and frequencies at only the initial and transition states and is therefore substantially less computationally intensive than methods that require these parameters along the entire minimum-energy reaction path (see ref 20 for further discussion). Results are expected to qualitatively predict the importance of including quantum tunneling in the overall proton-hopping rate. In addition, SC-TST has been applied to study proton mobility in zeolite clusters, thereby providing a useful comparison.²⁰ A crossover temperature, T_x , below which quantum tunneling dominates the proton-hopping rate and above which classical transitions dominate, is calculated as

$$T_x = \frac{\hbar|\omega|E_{\text{act}}/R}{2\pi E_{\text{act}}/N - \hbar|\omega|\ln 2} \quad (4)$$

Equation 4 is used to compare the importance of quantum tunneling in phosphotungstic acid to zeolite catalysts.

Results and Discussion

Anhydrous Proton-Hopping Reaction. The motion of protons on an isolated phosphotungstic acid Keggin unit is composed of a series of "hops" between oxygen atoms on the exterior surface. Three types of oxygen atoms are available to protons on the exterior of the Keggin structure and they are indicated in Figure 1. The two types of oxygen atoms that bridge between two tungsten atoms are labeled O_b and O_c . The terminal oxygen atoms, which bond to a single tungsten atom, are labeled O_d . Protons may move between oxygen atoms on the exterior

Table 1. DFT Optimized Interatomic Distances and Angles of the Equilibrium and Transition-State Structures for the Proton-Hopping Reaction between an O_c Atom and an O_d Atom of HPW^a

| | (a) initial H ⁺ on O_c | (b) transition state | (c) final H ⁺ on O_d |
|--|---|-------------------------|---|
| $\text{O}_c\text{--W--O}_d$ (deg) | 94.0 | 71.1 | 98.0 |
| $\text{H--O}_c\text{--W--O}_d$ (deg) | 17.1 | 0.6 | 0.3 |
| $\text{O}_c\text{--H}$ (Å) | 0.98 | 1.26 | 2.94 |
| $\text{O}_d\text{--H}$ (Å) | 2.80 | 1.25 | 0.98 |
| $\text{O}_c\text{--W}$ (Å) | 2.12 | 2.17 | 1.91 |
| $\text{O}_d\text{--W}$ (Å) | 1.71 | 1.80 | 1.85 |
| $\text{H}^+\text{--W}$ (Å) | 2.69 | 2.08 | 2.57 |
| W--P (Å) | 3.54 | 3.36 | 3.45 |
| $\text{O}_c\text{--H}^+\text{--O}_d$ (deg) | | 135.5 | |

^a (a), (b), and (c) refer to the corresponding structure labels in Figure 1.

of the Keggin unit through five different jump paths, three distinct paths between bridging oxygen atoms ($\text{O}_b\text{--O}_b$, $\text{O}_c\text{--O}_c$, $\text{O}_b\text{--O}_c$) and between either type of bridging oxygen atom and a terminal oxygen atom ($\text{O}_b\text{--O}_d$, $\text{O}_c\text{--O}_d$). The equilibrium position of a proton bound to a bridging O_c atom is calculated to be 0.3–0.5 Å closer to a nearby O_d atom than to a second bridging oxygen atom (i.e., O_b or O_c). The barrier for proton transfer between two bridging oxygen atoms would be significantly higher due to the larger distance over which transfer must occur. Therefore, the lowest-energy paths would be from bridging oxygen atoms to terminal oxygen atoms. Furthermore, transfer between either of the bridging oxygen atoms and a terminal oxygen atom is expected to be qualitatively similar. To simplify this study, only the jump path between an O_c atom and an O_d atom is investigated. As rotation about the O_d oxygen atom is likely facile, subsequent "hops" to other bridging oxygen atoms through similar jump paths allow the proton access to the entire KU exterior. This mechanism can be contrasted with studies of proton jump paths over zeolites. In zeolites, the activation barrier to proton hopping depends on whether the two oxygen atoms are connected to an aluminum or silicon atom and on the distance between the silicon and aluminum atoms.²⁹

The proton jump path considered here has the proton initially located on the O_c bridging oxygen atom and ending on the O_d terminal oxygen atom. The equilibrium and transition-state structures for this jump path are shown in Figure 1 with interatomic distances and angles listed in Table 1. Note that, although only a small section of the KU is shown in Figure 1(a,b,c), all calculations utilize the entire KU. In the initial state, the three protons are located at their optimal positions as previously determined.¹² The activation energy with reference to the equilibrium initial state is 117.9 kJ mol⁻¹. Zero-point vibrational energy corrections reduce the barrier to 103.3 kJ mol⁻¹. The imaginary frequency of the transition-state structure is 1513i cm⁻¹. The proton-hopping reaction energy is 12.9 kJ mol⁻¹, indicating that the O_c atom has a slightly higher proton affinity than the O_d atom, as previously reported.¹² The inclusion of ZPVE corrections reduces the reaction energy to 12.4 kJ mol⁻¹.

In the transition state, the proton is located equidistant between the O_c and O_d atoms. Substantial structural changes of the KU are required to reach this transition state. The $\text{O}_c\text{--W--O}_d$ angle closes from 94.0° to 71.1° to shorten the distance over which the proton is transferred and to stabilize the transition

(23) Kresse, G.; Furthmüller, J. *Phys. Rev. B* **1996**, *54*, 11169–11186.

(24) Vanderbilt, D. *Phys. Rev. B* **1990**, *41*, 7892–7895.

(25) Perdew, J. P.; Chevary, J. A.; Vosko, S. H.; Jackson, K. A.; Pederson, M. R.; Singh, D. J.; Fiolhais, C. *Phys. Rev. B* **1992**, *46*, 6671–7895.

(26) Monkhorst, H. J.; Pack, J. D. *Phys. Rev. B* **1976**, *13*, 5188–5192.

(27) Mills, G.; Jonsson, H.; Schenter, G. K. *Surf. Sci.* **1995**, *324*, 305–337.

(28) Ryder, J. A.; Chakraborty, A. K.; Bell, A. T. *J. Phys. Chem. B* **2000**, *104*, 6998–7011.

(29) Franke, M. E.; Sierka, M.; Simon, U.; Sauer, J. *Phys. Chem. Chem. Phys.* **2002**, *4*, 5207–5216.

Table 2. Comparison of Activation Barriers (E_{act}), Reactive Mode Frequencies (ν_{F}), and Quantum-Tunneling Crossover Temperatures (T_{x}) for the Proton-Hopping Reaction in Zeolites and Phosphotungstic Acid

| source | solid acid | E_{act} (kJ mol ⁻¹) | ν_{F} (cm ⁻¹) | T_{x} (K) |
|----------------------------------|---------------------------------|--|--------------------------------------|--------------------|
| Ryder et al. ²⁸ | H-ZSM-5 | 117.2 | 1785 | 417 |
| Fermann et al. ³⁰ | H-Y Zeolite | 97.1 | 1570 | 368 |
| Sierka and Sauer ^{a,31} | chabazite, faujasite, and ZSM-5 | 68.3–105.8 | 760–1369 | 184–320 |
| this work | phosphotungstic acid | 103.3 | 1513 | 353 |

^a Sierka and Sauer³¹ studied transitions between various pairs of oxygen atoms within each of the zeolite structures. Ranges are over all the structures and all oxygen atom pairs considered.

state. This primarily involves a tilt of the W–O_d bond away from its equilibrium position in the octahedron toward the transferring proton. The adjacent tungsten atom contracts into the KU structure, indicated by a shorter tungsten–phosphorus distance. These structural rearrangements allow the proton to pass along a hydrogen bond between the O_c and O_d atoms rather than through an isolated state. However, the activation energy required to facilitate these structural rearrangements is substantial. Furthermore, the geometry does not allow for effective hydrogen bonding. The O_c–H–O_d angle is 135°, which is far from the ideal 180° angle typical for proton transfer through hydrogen-bonded water networks. This case is contrasted with proton transfer between two Keggin units in an ideal one-dimensional lattice, where KUs are aligned to allow for a strong and linear hydrogen bond between O_d atoms on two KUs. Proton transfer along the linear hydrogen bond, with little KU structural rearrangement, has a negligible activation barrier.¹⁵

The harmonic vibrational frequencies were calculated by displacing only a subset of the atoms of the KU from their equilibrium or transition-state positions. Because a finite convergence criterion is used in locating the optimum nuclei positions, the forces on all atoms at the equilibrium geometries are not exactly zero. Therefore, a subset of the vibrational degrees of freedom are not precisely in the basin of the potential-energy well. Due to the size of the system, many of the low-energy “structural” modes of the Keggin unit are calculated to have negative force constants, and the number of these modes may differ between the initial, transition, and final states. Furthermore, with the inclusion of periodic boundary conditions, 168 harmonic modes are calculated for the 56-atom system. This includes the 162 vibrational modes and the 6 translational and rotational degrees of freedom. Within the periodic code, it is difficult to distinguish the six molecular translational and rotational modes from the low-energy vibrational modes. We therefore used constrained vibrational calculations to help avoid such difficulties. Approximations however are clearly introduced which differ on the basis of the choice of atoms to displace in the initial, transition, and final states.

Vibrational frequencies were calculated for three purposes: to determine the ZPVE corrections to the activation and reaction energies, to identify the imaginary frequency associated with the reactive mode for quantum-tunneling calculations, and to determine vibrational partition functions for the preexponential factor of the rate constant. The ZPVE corrections are dominated by the changes in the high-energy modes and are only slightly affected by any changes to low-energy KU structural modes. These changes can be captured reasonably well by including the proton, the O_c atom to which the proton is initially bound, and the O_d atom to which the proton is bound in the final state in the vibrational calculation. Calculation of the reactive mode frequency requires the inclusion of more atoms, as local

structural rearrangement of the tungsten atoms bound to the O_c and O_d atoms occurs along the reaction coordinate. Vibrational partition functions are dominated by the low-energy modes at the temperatures of interest, and therefore their values are only approximate without including the entire KU. The vibrational partition functions for the initial and transition states are calculated with the same number of atoms. However, one less vibrational mode is included in the transition-state partition function due to the loss of a vibrational degree of freedom along the reaction coordinate. Values reported from vibrational calculations were determined for displacements of the six atoms illustrated in the magnified views of Figure 1: the mobile proton, the O_c atom to which it is initially bound, the two adjacent tungsten atoms, and the two nearest O_d atoms. The ratio of the transition-state to the initial-state partition functions converges within an order of magnitude with respect to including more atoms in the vibrational calculation.

The activation barrier, E_{act} , and reactive-mode frequency, ν_{F} , are used via eq 4 to determine the crossover temperature, T_{x} , below which quantum-tunneling transitions dominate and above which classical transitions gain in importance. The crossover temperature for the proton-hopping reaction on the KU is calculated to be 353 K. The values of E_{act} , ν_{F} , and T_{x} are compared in Table 2 with the proton-hopping reactions between two oxygen atoms of an AlO₄ tetrahedron within various zeolite structures, calculated from the literature. Generally, the activation energy for the proton-hopping reaction determined for phosphotungstic acid (103.3 kJ mol⁻¹) is similar to that found for zeolites (68.3–117.2 kJ mol⁻¹).^{28,30,31} The crossover temperature (353 K) is best compared with the work of Sierka and Sauer (184–320 K)³¹ since they take the periodic lattice into account. The crossover temperature for phosphotungstic acid is 33 K higher than the highest calculated temperatures in their zeolite structures. Apparently, quantum-tunneling transitions are more important at temperatures of interest for phosphotungstic acid. At the crossover temperature, the quantum-tunneling correction factor, $\Gamma(353 \text{ K})$, is 25.4 (eq 3). The crossover temperature, therefore, does not represent a sharp transition between the two mechanisms but rather a point where the relative dominance is rapidly changing.²⁰

Reaction rate constants calculated from eqs 1 and 3 at various temperatures are listed in Table 3, expressed on a per proton basis. The rate constant is calculated up to 600 K, the upper limit of Keggin unit stability.³² The k^{TST} values are generally an order of magnitude higher than those calculated by Ryder et al. for H-ZSM-5 because of the lower activation energy for

(30) Fermann, J. T.; Blanco, C.; Auerbach, S. *J. Chem. Phys.* **2000**, *112*, 6779–6786.

(31) Sierka, M.; Sauer, J. *J. Phys. Chem. B* **2001**, *105*, 1603–1613.

(32) Fournier, M.; Feumi-Jantou, C.; Rabia, C.; Herve, G.; Launay, S. *J. Mater. Chem.* **1992**, *2*, 971–978.

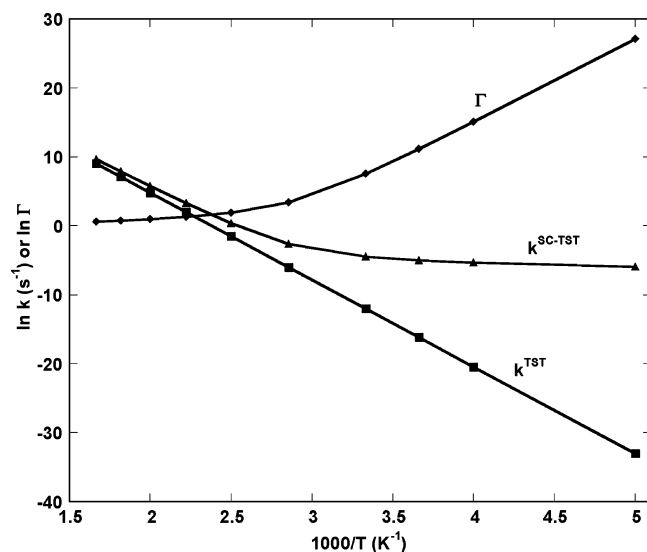


Figure 2. Arrhenius plot of $k^{\text{TST}}(T)$, $k^{\text{SC-TST}}(T)$, and $\Gamma(T)$ for the anhydrous proton-hopping reaction from an O_c atom to an O_d atom of HPW.

Table 3. Calculated Rate Constants for the Anhydrous Proton-Hopping Reaction from an O_c Atom to an O_d Atom of HPW

| T (K) | A (s^{-1}) | k^{TST} (s^{-1}) | Γ | $k^{\text{SC-TST}}$ (s^{-1}) |
|---------|-------------------------|--------------------------------------|-----------------------|---|
| 200 | 4.16×10^{12} | 4.43×10^{-15} | 5.96×10^{11} | 2.64×10^{-3} |
| 250 | 4.97×10^{12} | 1.32×10^{-9} | 3.65×10^6 | 4.80×10^{-3} |
| 273 | 5.31×10^{12} | 9.46×10^{-8} | 7.13×10^4 | 6.74×10^{-3} |
| 300 | 5.66×10^{12} | 5.91×10^{-6} | 1.91×10^3 | 1.13×10^{-2} |
| 350 | 6.23×10^{12} | 2.41×10^{-3} | 2.98×10^1 | 7.18×10^{-2} |
| 400 | 6.72×10^{12} | 2.19×10^{-1} | 6.61×10^0 | 1.45×10^0 |
| 450 | 7.14×10^{12} | 7.35×10^0 | 3.66×10^0 | 2.69×10^1 |
| 500 | 7.51×10^{12} | 1.22×10^2 | 2.65×10^0 | 3.23×10^2 |
| 550 | 7.84×10^{12} | 1.22×10^3 | 2.16×10^0 | 2.63×10^3 |
| 600 | 8.14×10^{12} | 8.32×10^3 | 1.87×10^0 | 1.56×10^4 |

phosphotungstic acid. A fit of k^{TST} to an Arrhenius form gives an apparent activation energy of $105.0 \text{ kJ mol}^{-1}$.

Quantum-tunneling transitions are important over the entire temperature range considered. Figure 2 illustrates the significance of quantum tunneling to the proton-hopping reaction rate. At low temperatures the rate constant for proton hopping is nearly temperature independent since quantum tunneling dominates. At higher temperatures, classical transitions dominate. As a result of quantum tunneling, an Arrhenius fit of the rate data will predict very different activation energies, depending on the temperature range studied. For example, the values of $k^{\text{SC-TST}}$ from 200 to 350 K give an apparent activation energy of 11.6 kJ mol^{-1} , whereas values of $k^{\text{SC-TST}}$ from 400 to 600 K give an apparent activation energy of 92.7 kJ mol^{-1} .

Since the reaction is not thermoneutral, the reverse reaction has a different rate, which is generally an order of magnitude higher because the activation energy is 12 kJ mol^{-1} lower. The value of $\Gamma(T)$, and hence the preference of the quantum-tunneling mechanism, is strongly dependent on the curvature of the barrier and only slightly affected by a change of the activation energy.²⁰ The rate-limiting step for proton movement on a single KU is the hop from the bridging to the terminal oxygen atom, followed by a more rapid return to a bridging oxygen atom.

Water-Assisted Proton-Hopping Reaction. To evaluate the impact of water on proton mobility, the mechanism of water-assisted proton hopping was explored. The adsorption of water

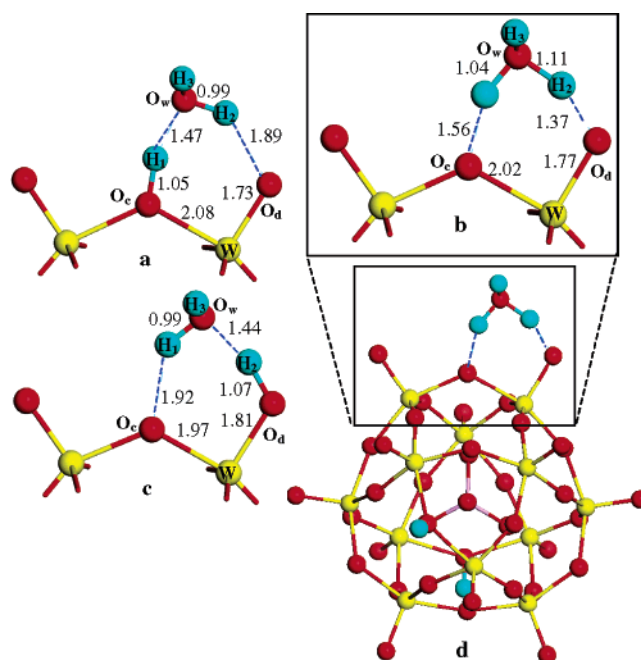


Figure 3. DFT calculated equilibrium states and transition state for the water-assisted proton-hopping reaction between an O_c atom and an O_d atom. (a) Equilibrium structure with H_2O adsorbed to a H^+ on an O_c atom. (b) Transition state for the water-assisted proton-hopping reaction between O_c and O_d atoms. (c) Equilibrium structure with H_2O adsorbed to a H^+ on an O_d atom. (d) Full Keggin unit view of the transition state. All calculations were performed on the full Keggin unit. The ZPVE corrected activation energy for movement starting on the O_c atom is 11.2 kJ mol^{-1} . Distances are given in Å.

molecules on the acidic protons of the phosphotungstic KU is exothermic with adsorption energies ranging from -55 to -70 kJ mol^{-1} , depending on the proton location.¹² Monodentate and bidentate water adsorption modes are possible. For monodentate adsorption, a hydrogen bond is formed between the proton on the KU and the oxygen atom of the water molecule. Bidentate water adsorption includes formation of a second hydrogen bond between a hydrogen atom of the water molecule and a second oxygen atom of the KU. For the adsorption of water on a proton residing on an O_c atom, the bidentate form is preferred by 4.9 kJ mol^{-1} . The adsorption energy of water at this site is $-62.9 \text{ kJ mol}^{-1}$, or -51 kJ mol^{-1} with ZPVE corrections included. For water adsorption at the terminal site (proton on O_d atom), only a bidentate-adsorption mode was identified. The adsorption energy of water at this site is $-60.6 \text{ kJ mol}^{-1}$ without ZPVE corrections.

With water adsorbed, proton hopping proceeds through a “rocking” mechanism. The bond between the proton and the O_c atom is lengthened as the H-O_d bond is shortened. The initial-site hydrogen bond angle decreases while the final-site hydrogen bond angle increases to be closer to the ideal 180° . The equilibrium and transition states for this reaction are shown in Figure 3, with interatomic distances and angles given in Table 4. The transition state appears as a separated hydronium ion with hydrogen bonds to the two oxygen atom sites of the KU. The activation barrier for this transfer is 19.1 kJ mol^{-1} , with ZPVE corrections reducing the barrier to 11.2 kJ mol^{-1} . The transition state has a single imaginary vibrational frequency of $303i \text{ cm}^{-1}$. The potential-energy surface along the reaction coordinate is more level than that of anhydrous proton hopping. Only the proton, O_c and O_d atoms, adjacent tungsten atom, and

Table 4. DFT Optimized Interatomic Distances and Angles of the Equilibrium and Transition-State Structures for the Water-Assisted Proton-Hopping Reaction between an O_c Atom and an O_d Atom of HPW^a

| | (a) initial H ₃ O ⁺ on O _c | (b) transition state | (c) final H ₃ O ⁺ on O _d |
|--|--|-------------------------|--|
| O _c –H ₁ –O _w (deg) | 162.9 | 151.9 | 137.5 |
| O _d –H ₂ –O _w (deg) | 140.1 | 156.4 | 162.8 |
| O _c –H ₁ (Å) | 1.05 | 1.56 | 1.92 |
| O _w –H ₁ (Å) | 1.47 | 1.04 | 0.99 |
| O _w –H ₂ (Å) | 0.99 | 1.11 | 1.44 |
| O _d –H ₂ (Å) | 1.89 | 1.37 | 1.07 |
| O _w –H ₃ (Å) | 0.97 | 0.98 | 0.98 |
| O _c –W (Å) | 2.08 | 2.02 | 1.97 |
| O _d –W (Å) | 1.73 | 1.77 | 1.81 |

Table 5. Calculated Rate Constants for the Water-Assisted Proton-Hopping Reaction from an O_c Atom to an O_d Atom of HPW

| T (K) | A (s ⁻¹) | k ^{TST} (s ⁻¹) | T (K) | A (s ⁻¹) | k ^{TST} (s ⁻¹) |
|-------|-------------------------|-------------------------------------|-------|-------------------------|-------------------------------------|
| 200 | 4.45 × 10 ¹² | 5.15 × 10 ⁹ | 400 | 6.25 × 10 ¹² | 2.13 × 10 ¹¹ |
| 250 | 5.12 × 10 ¹² | 2.29 × 10 ¹⁰ | 450 | 6.46 × 10 ¹² | 3.20 × 10 ¹¹ |
| 273 | 5.36 × 10 ¹² | 3.80 × 10 ¹⁰ | 500 | 6.63 × 10 ¹² | 4.44 × 10 ¹¹ |
| 300 | 5.61 × 10 ¹² | 6.19 × 10 ¹⁰ | 550 | 6.77 × 10 ¹² | 5.79 × 10 ¹¹ |
| 350 | 5.97 × 10 ¹² | 1.25 × 10 ¹¹ | 600 | 6.89 × 10 ¹² | 7.23 × 10 ¹¹ |

atoms of the water molecule were displaced in determining the vibrational frequencies.

Water-assisted proton hopping between the O_c and O_d sites occurs by the movement of two hydrogen atoms along hydrogen bonds. Little structural arrangement of the KU is required in this process. The O_c–W–O_d angle reduces only slightly from 92.3° in the initial state to 91.0° in the transition state, and the W–P distance is virtually unchanged (Table 4). The presence of water has reduced the activation barrier to proton movement by an order of magnitude compared to that for the anhydrous process.

The rate constant for water-assisted proton hopping was calculated at various temperatures using eq 2 and is summarized in Table 5. The apparent activation energy using an Arrhenius expression is 12.3 kJ mol⁻¹. The water-assisted proton-hopping rate is 7–10 orders of magnitude greater than the anhydrous hopping rate, indicating that small amounts of water will have large effects on the overall proton mobility. To better understand the effects of water on the proton-hopping rate and the impact of changes in the water adsorption equilibrium with temperature, the adsorption equilibrium constant is calculated from

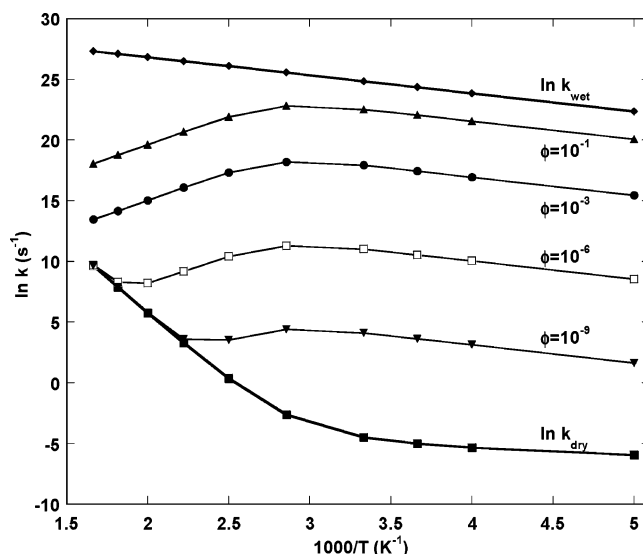
$$K_{\text{ads}} = \frac{Nq_{\text{H}_3\text{O}^+-\text{bridge,vib}}}{q_{\text{H}_2\text{O,trans}}q_{\text{H}_2\text{O,rot}}q_{\text{H}_2\text{O,vib}}q_{\text{H}^+-\text{bridge,vib}}} e^{(-E_{\text{ads}}/RT)} \quad (5)$$

where $q_{\text{H}_2\text{O,trans}}$, $q_{\text{H}_2\text{O,rot}}$, and $q_{\text{H}_2\text{O,vib}}$ are the translational, rotational, and vibrational partition functions for a gas-phase water molecule and E_{ads} is the ZPVE corrected water adsorption energy.

The fraction of sites covered with water molecules is determined using the Langmuir isotherm

$$\theta = \frac{K_{\text{ads}}P_{\text{H}_2\text{O}}}{1 + K_{\text{ads}}P_{\text{H}_2\text{O}}} \quad (6)$$

where θ is the fraction of protons with water molecules adsorbed and $P_{\text{H}_2\text{O}}$ is the partial pressure of water in the gas phase. The

**Figure 4.** Arrhenius plot of the overall rate of proton hopping versus temperature with different amounts of water in the environment. The value ϕ is defined as the moles of water in the system per proton in the HPW sample.

rate constant for proton hopping is a combination of the water-assisted and anhydrous hopping rates, expressed as

$$k = (1 - \theta)k_{\text{dry}} + \theta k_{\text{wet}} \quad (7)$$

The fractional coverage was determined by assuming a constant volume system with 0.1 g of phosphotungstic acid in a system volume of 1 cm³ at 1 atm total pressure. This model represents an ideal situation in which all water molecules adsorb only to isolated protons. The formation of a secondary structure involving hydrate proton bridges between Keggin units is not considered. A value ϕ is defined as the ratio of moles water in the system to moles protons in the sample. The amount of water in the system, given by ϕ , is kept constant for a series of rate calculations rather than the amount in the gas phase. The gas-phase partial pressure can be calculated as

$$P_{\text{H}_2\text{O}} = \frac{(\phi - \theta)(\text{mol H}^+)RT}{V} \quad (8)$$

This expression for the gas-phase partial pressure is substituted into eq 6. At a ϕ value of 10⁻⁶, the equilibrium partial pressure of water in the gas phase at 300 K is calculated to be 5.83 × 10⁻⁸ atmospheres.

Figure 4 presents the rate of the proton-hopping reaction versus temperature for various amounts of water in the system. At low temperatures (below 350 K) the rate of proton hopping is dominated by water-assisted transitions, as seen by the substantially greater rate over k_{dry} for $\phi > 0$. Even the presence of water at 1 ppm drastically increases the proton-hopping rate so that 99.996% of proton-hopping reactions are water-assisted at 400 K. At approximately 350 K, the rate of proton hopping begins decreasing with increasing temperature because of water desorption. For water present in the ppm range, this trend continues to temperatures greater than 500 K. A negative apparent activation energy for proton hopping would be measured over this temperature range since the equilibrium amount of adsorbed water decreases with increased temperature. Because larger amounts of water lead to a secondary structure

with protons located in H_5O_2^+ bridges between KUs, the high water coverage values in Figure 4 must be considered hypothetical.

Relevance of Proton Hopping. The adsorption of water substantially reduces the energy barrier to proton hopping by providing a pathway that does not require substantial structural rearrangement of the Keggin unit to form the transition state. The presence of water, even in extremely low pressures, dictates that virtually all proton movement will be as a hydrated species. These findings can be used to provide additional insights into previous experimental studies of proton mobility and to the applications of HPAs as acid catalysts and as additives in proton exchange membranes. First, the results of this study are placed in context with similar studies of the proton-hopping reaction in zeolites.

The reaction paths and activation energies for anhydrous and water-assisted proton transfer on the exterior of the phosphotungstic Keggin unit are very similar to those found for the same process on zeolites. The activation energies for anhydrous proton hopping on HPW are in the range of those found on zeolites for the proton-hopping reaction between oxygen atoms of an aluminum tetrahedron ($68.3\text{--}117.2\text{ kJ mol}^{-1}$, Table 2).^{28,30,31} Zeolite studies also indicate a similar reaction path to HPAs, in which the O–M–O angle narrows to shorten the distance over which the proton is transferred. The reaction path and activation energy for water-assisted proton transfer over HPW is also similar to that found in computational studies of zeolitic clusters, which identify the hydronium ion as the transition state with activation energies of $<20\text{ kJ mol}^{-1}$.^{33,34} As the composition (tungsten versus aluminum) and geometry (octahedral versus tetrahedral) of the two solid acids differ, the qualitative and quantitative similarities are not obvious. However, because the KU structure differs substantially from that of zeolites, the consequences of proton mobility are not identical. The same jump path over the KU allows access to the entire exterior surface, while the proton-hopping reaction in zeolites allows only movement between oxygen atoms of the same aluminum tetrahedron. Franke et al. found that for H-ZSM-5 Brønsted sites separated by 14 \AA , the highest energy barrier to movement between the sites is 210 kJ mol^{-1} above the initial and final equilibrium-state energies, substantially greater than the barrier for movement between two oxygen atoms on the same aluminum tetrahedron.²⁹

The results of this study provide insight into experimental studies of proton mobility with low amounts of water, in which the vehicle mechanism of proton transport is expected to dominate. In the vehicle mechanism, water assists proton movement by facilitating transport as an H_3O^+ species. This differs from the Grotthaus mechanism, in which large amounts of water can assist proton transport through a hydrogen-bonded network. Conductivity studies and NMR characterization of HPW provide experimental evidence of the effect of water on the proton mobility. The trends for the influence of temperature on the proton-hopping rate found here are analogous to those observed in conductivity experiments. The conductivity of $\text{HPW}\cdot 6\text{H}_2\text{O}$ increases with temperature up to 453 K until dehydration becomes important, causing a conductivity decrease

with temperature. After complete dehydration, the conductivity again increases over a small temperature range until decomposition of the KU occurs.³⁵ These results suggest a balance between the increased rate of proton motion with temperature and the shift in the water adsorption equilibrium. Baba and Ono used ^1H MAS NMR for low levels of hydration (<1 water molecule per KU) to show the rapid exchange of protons between the acid and adsorbed water.¹⁶ This exchange can be taken as an indication of mobility, as each water-assisted hop changes which hydrogen atom of H_3O^+ interacts strongest with the KU. Uchida et al. showed with variable temperature ^{31}P MAS NMR of $\text{H}_3\text{-PW}_{12}\text{O}_{40}\cdot 2.1\text{H}_2\text{O}$ that separate peaks for KUs with one, two, or three isolated protons coalesced at room temperature into a single broad peak.³⁶ The authors concluded that in the presence of water, protons were mobile between KUs at 298 K at a rate faster than 200 Hz . Experimental studies are not able to separate proton motion around a single KU from the transfer of protons between KUs.

The motion of protons between KUs is essential to the process of proton conduction and may impact catalytic properties as well. This study examined only the motion of protons between oxygen atoms on a single KU. Previously, we showed that there is a substantial energy advantage for an anhydrous proton to form a hydrogen bond with an adjacent KU on the order of -43 to -71 kJ mol^{-1} per proton “shared”, depending on the relative geometry of the two KUs.¹⁵ In addition, the movement of the proton along the hydrogen bond between the two KUs was found to have a negligible activation barrier. This shared position provides a stable low-energy well for the proton. The reaction coordinate for hopping out of this well to an adjacent oxygen atom requires breaking the hydrogen bond along with the KU structural rearrangements necessary to bring the two oxygen atoms together. Therefore, the activation energy is expected to increase by an amount at least on the order of the strength of the hydrogen bond. Proton movement out of this well is likely the slowest process in anhydrous proton motion.

Protons in shared positions between KUs are also likely to be considerably less active for acid-catalyzed reactions that inherently begin with the donation of electron density from the reactant molecule to the proton. Because the “shared” proton position is more stable, the proton affinity is higher and the acid strength is reduced. In addition, the access of reactant hydrocarbons to protons located between KUs is sterically hindered. Finally, protons participating in a strong hydrogen bond to an electron-donating oxygen atom of an adjacent KU are less likely to interact in this manner with a reactant molecule.

By increasing proton mobility, water may facilitate the movement of protons out of inactive low-energy wells, increasing the time spent in active positions. The energy advantage for an H_3O^+ species to bridge between adjacent KUs was found to be substantially lower than that for a proton. Because bidentate adsorption of H_3O^+ on a single KU is already preferred and no additional hydrogen bonds are formed by binding to a second KU, proton hydration may facilitate the distribution of protons among shared positions and positions on a single KU. As already shown for proton mobility on a single KU, small amounts of water greatly enhance the proton-hopping rate.

(33) Krossner, M.; Sauer, J. *J. Phys. Chem.* **1996**, *100*, 6199–6211.

(34) Zygmunt, S. A.; Curtiss, L. A.; Iton, L. E.; Erhardt, M. K. *J. Phys. Chem.* **1996**, *100*, 6663–6671.

(35) Slade, R. C. T.; Omana, M. J. *Solid State Ionics* **1992**, *58*, 195–199.

(36) Uchida, S.; Inumaru, K.; Misono, M. *J. Phys. Chem. B* **2000**, *104*, 8108–8115.

Therefore, a low number of water molecules at adsorption equilibrium may enhance the time protons spend in “active” locations (i.e. bound to a single KU) while still allowing for a high probability of reactant molecules to encounter active anhydrous protons.

Conclusions

The activation energies and reaction energies for both anhydrous and water-assisted proton hopping over phosphotungstic acid were determined using density functional theory quantum-chemical methods. The adsorption of water on the acidic protons of phosphotungstic acid decreases the barrier with respect to anhydrous proton movement by an order of magnitude, from 103.3 kJ mol⁻¹ to 11.2 kJ mol⁻¹. The inclusion of quantum tunneling in the rate expression considerably affects the rate of anhydrous proton hopping below about 350 K. The molecular-level results were used to calculate the overall proton-hopping rate as a function of temperature and water partial

pressure. Small amounts of water greatly increase the overall rate of proton movement, with 99.996% of proton-hopping reactions being water-assisted at 400 K and ppm levels of gas-phase water. The proton-hopping rate increases with temperature in the presence of water until the shift in the water adsorption equilibrium leads to a decreasing rate due to dehydration.

Acknowledgment. We thank Kimberly Campbell and Dr. Billy Bardin for helpful discussions, the National Science Foundation (CTS-0124333) for financial support, and the Environmental Molecular Science Laboratory (Project 3568) at Pacific Northwest Laboratories for computational resources.

Supporting Information Available: Geometries (in Cartesian coordinates) and computed absolute energies for structures illustrated in Figures 1 and 3. This material is available free of charge via the Internet at <http://pubs.acs.org>.

JA042742O